Secretome Profiling of Primary Cells Reveals That THBS2 Is a Salivary Biomarker of Oral Cavity Squamous Cell Carcinoma

ARTICLE *in* JOURNAL OF PROTEOME RESEARCH · APRIL 2014

Impact Factor: 4.25 · DOI: 10.1021/pr500038k · Source: PubMed

Journal of proteome research

Article

pubs.acs.org/jpr

Secretome Profiling of Primary Cells Reveals That THBS2 Is a Salivary Biomarker of Oral Cavity Squamous Cell Carcinoma

Chia-Wei Hsu,[†,¶] Jau-Song Yu,[†,‡,∥] Pei-Hua Peng,[∥] Shu-Chen Liu,[∥] Yu-Sun Chang,[∥] Kai-Ping Chang,*[,∥,⊥] and Chih-Ching Wu*[,†,§,∥,¶]

[†]Graduate Institute of Biomedical Sciences, College of Medicine, [‡]Department of Cell and Molecular Biology, College of Medicine, [§]Department of Medical Biotechnology and Laboratory Science, College of Medicine, and [∥]Molecular Medicine Research Center, Chang Gung University, Tao-Yuan, Taiwan

[⊥]Department of Otolaryngology-Head & Neck Surgery, Chang Gung Memorial Hospital, Lin-Kou, Taiwan

Supporting Information

ABSTRACT: Oral cavity squamous cell carcinoma (OSCC), which is a leading cause of cancer-related death worldwide, is frequently associated with poor prognosis and mortality. The discovery of body fluid-accessible biomarkers may help improve the detection of OSCC. In the present work, we established primary cell cultures derived from OSCC and adjacent noncancerous epithelium and performed comparative profiling of their secretomes. Using spectral counting-based label-free quantification, we found that 64 proteins were significantly higher in primary OSCC cells compared with primary adjacent noncancerous cells. We then retrieved the mRNA expression levels of these 64 proteins in oral cavity tumor and noncancerous tissues from public domain array-based transcriptome data sets and used this information to prioritize the biomarker candidates. We identified 19 candidates; among them, the protein levels of THBS2, UFD1L, and DNAJB11 were found to be elevated in OSCC tissues compared with adjacent noncancerous epithelia. Importantly, higher levels of THBS2 in OSCC tissues were associated with a higher overall pathological stage, positive perineural invasion, and a poorer prognosis. Moreover, the salivary levels of THBS2 in OSCC patients were elevated compared to those of noncancer controls. Our results collectively indicate that analysis of the primary cell secretome is a feasible strategy for biomarker identification, and that THBS2 is a potentially useful salivary marker for the detection of OSCC.

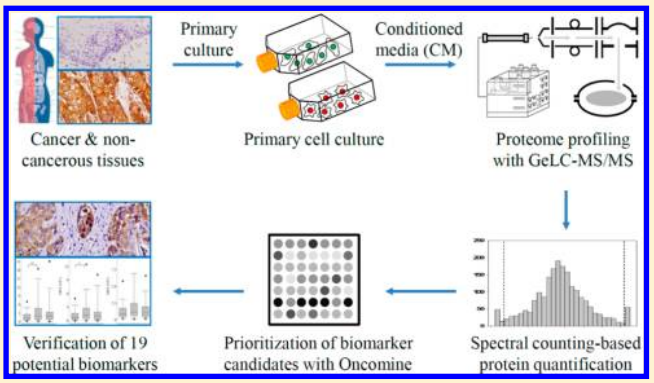

KEYWORDS: *thrombospondin-2, biomarker, saliva, secretome, oral cavity squamous cell carcinoma, primary cell*

INTRODUCTION

Oral cavity squamous cell carcinoma (OSCC), the most common malignancy of the head and neck, accounts for nearly 3% of annual cancer incidence and death worldwide.[1] OSCC is a destructive disease; despite recent advances in the treatment options, approximately 50% of OSCC patients die within 5 years after the initial diagnosis.[2] The disappointing outcome among OSCC patients largely reflects that the disease is often quite advanced at the time of diagnosis,[3] suggesting that early detection of the disease is needed to improve the treatment outcome and reduce the growing burden of OSCC.[4] The use of noninvasive body-fluid-accessible biomarkers may represent an effective tool for the early detection of this disease. To date, however, no effective biomarker has been approved for the diagnosis and/or prognosis of OSCC.

Secretome profiling of cancer cell lines is a promising strategy for discovering potential cancer biomarkers.[5−8] Our group and others have demonstrated that secretome-based strategies are effective in a variety of cancer types, including gastric cancer,[9] lung cancer,[10,11] ovarian cancer,[12,13] colon cancer,[14,15] breast cancer,[16] pancreatic cancer,[17] nasopharyngeal carcinoma,[8,18] and head-neck cancer.[19] As the numbers of identified proteins increase through the secretome analyses of various cancer cell lines, scientists are confronted with the challenge of efficiently choosing candidates that may have higher chances of success in subsequent clinical validation studies. Theoretically, the best way to do this is to generate the secretome data set from a corresponding noncancerous cell lines and perform comparisons. However, noncancerous cell lines are rarely available. In the previous studies, therefore, marker candidates were often selected by integrating the obtained data with those from other omics-related analyses, such as cancer-related body fluid proteomes,[10−14] tissue

Special Issue: Proteomics of Human Diseases: Pathogenesis, Diagnosis, Prognosis, and Treatment

Received: January 7, 2014

dx.doi.org/10.1021/pr500038k | J. Proteome Res. XXXX, XXX, XXX−XXX

Table 1. Characteristics of Tissue Samples Used for Primary Cell Culture

patient ID	tissue type	sex	age (years)	site	TNM stage	cell differentiation
1[a]	adjacent normal	male	51	tongue		
2[b]	cancerous	male	51	floor of mouth	T2N0M0	moderate
3[b]	cancerous	male	43	buccal mucosa	T2N0M0	moderate

[a]The establishment of primary cancer cells in patient 1 failed. The cancer was diagnosed at the stage of T4N0M0 and as moderate differentiation. [b]The primary adjacent noncancerous cells of the patient failed to be established.

transcriptomes,[16−18] and the Human Protein Atlas.[8,19] In a previous effort to identify OSCC biomarkers, we analyzed the OSCC cell line secretome and compared our list of potential candidates with the tissue transcriptomes of OSCC and normal tissues. We selected GBP1 for further biomarker evaluation based on the observation that it was significantly elevated in the OSCC tissue transcriptome. We then confirmed that the serum level of GBP1 is elevated in OSCC patients.[20]

Regarding the discovery of useful biomarkers, there are other potential problems with using cancer cell lines for secretome analysis. For example, numerous cancer cell lines have been cultured *in vitro* for many generations since their initial establishment, and the expression levels of genes and proteins in cancer cell lines may be altered in response to the culture environment.[21,22] Thus, the secretome of a given cancer cell line may not be representative of the proteins released from the corresponding cancer cells *in vivo*. In addition, the proteins identified in the secretome of cancer cells may also be released from the relevant noncancerous cells.

To circumvent these problems, we herein established primary cell cultures derived from OSCC and adjacent noncancerous epithelium tissues. The proteins in conditioned media from primary cultured cells were detected using SDS-PAGE coupled with liquid chromatography-tandem mass spectrometry (GeLC−MS/MS). Spectral counting-based label-free quantification showed that the levels of 64 proteins were increased in primary OSCC cells compared with primary adjacent noncancerous cells. We retrieved the mRNA expression levels of these 64 proteins in oral cavity tumor and noncancerous tissues from public domain array-based transcriptome data sets and used this information to prioritize the biomarker candidates. Among the isolated candidates, thrombospondin-2 (THBS2) was found to be significantly elevated in OSCC tissues compared with adjacent noncancerous epithelia. Higher levels of THBS2 in cancer tissue were associated with a poorer prognosis among OSCC patients. More importantly, the salivary levels of THBS2 were significantly higher in OSCC patients compared to healthy controls and subjects with oral potentially malignant disorder (OPMD). Our results collectively indicate that analysis of the secretome of primary oral epithelial cells is a feasible strategy for OSCC biomarker identification, and that THBS2 is a potentially useful salivary marker for the detection of OSCC.

MATERIALS AND METHODS

Patient Populations and Clinical Specimens

The tissues used for the establishment of primary cell cultures were collected from three OSCC patients diagnosed at the Chang Gung Memorial Hospital (Taoyuan, Taiwan) in 2010 (Table 1). The tumor specimens used for immunohistochemical analysis were obtained from 160 OSCC patients diagnosed at the Chang Gung Memorial Hospital from 2002 to 2008. The demographic data for these patients are shown in Table 3. Saliva samples were collected from 47 healthy volunteers, 47 individuals with OPMD, and 49 OSCC patients seen at the Chang Gung Memorial Hospital from 2012 to 2013. All volunteers were examined by an oral mucosal screening test. The cases of OPMD and OSCC were biopsy-proven, and patients underwent routine check-ups according to standard protocols. This research followed the tenets of the Declaration of Helsinki. All subjects signed an informed consent form approved by the Institutional Review Board of Chang Gung Memorial Hospital prior to participation and/or the use of previously collected saliva samples.

For the collection of saliva samples, the donors avoided eating, drinking, smoking, and using oral hygiene products for at least 1 h before collection, and unstimulated whole saliva was obtained during oral mucosal examination. The collected samples were centrifuged at 3000 × *g* for 15 min at 4 °C. The supernatants were immediately treated with a protease inhibitor mixture (2 μL/mL; Sigma-Aldrich, St. Louis, MO, USA) and, aliquoted into smaller volumes, and stored at −80 °C. To avoid issues with protein degradation, we did not reuse thawed saliva samples.

Culture of Primary Cells and OSCC Cell Lines

For primary cell cultures, OSCC and adjacent noncancerous tissues were collected from three OSCC patients. The collected samples were soaked in cold Dulbecco's modified Eagle's media (DMEM; Invitrogen, Carlsbad, CA, USA) containing 10 μg/mL gentamicin and 2 μg/mL amphotericin B (Invitrogen) and processed within 30 min after surgery. The tissue samples were washed three times with ice-cold PBS containing gentamicin, cut into small pieces (1 mm^3), and incubated with 0.05% trypsin (Invitrogen) at 37 °C for 20 min under low agitation. The explants were then distributed atop heavily irradiated NIH/3T3 feeder layers in DMEM supplemented with 10% FBS (Biological Industries, Israel), 10 μg/mL gentamicin, and 2 μg/mL amphotericin B (Invitrogen). As epithelial outgrowths from the explants were observed, cells were fed with defined keratinocyte serum-free medium (K-SFM; Invitrogen) to stimulate the proliferation of epithelial cells. When epithelial outgrowths reached preconfluence, cells were trypsinized and seeded onto collagen-coated culture vessels for subsequent passages, prior to the onset of terminal differentiation. The third to sixth passages of preconfluent primary epithelial cells were used for experiments. The methods used for immunofluorescent staining of cytokeratins and Thy-1 in the primary cell cultures are described in the Supplemental Materials and Methods. OEC-M1 cells were cultured in RPMI 1640 (Invitrogen) supplemented with 10% FBS. SCC25 cells were maintained in DMEM/F-12 (Invitrogen) supplemented with 10% FBS. OC3 cells were maintained in DMEM supplemented with 10% FBS and K-SFM (1:2 ratio). SAS cells were cultured in DMEM supplemented with 10% FBS. All cells were cultured at 37 °C in a humidified incubator containing 5% CO_2.

dx.doi.org/10.1021/pr500038k | J. Proteome Res. XXXX, XXX, XXX−XXX

Harvest of Conditioned Media and Cell Extracts

Conditioned media and cell extracts were collected and processed as described in the Supplemental Materials and Methods.

SDS-PAGE and In-Gel Protein Digestion

Proteins (20 and 50 μg for primary cells and cancer cell lines, respectively) from the conditioned media and cell extracts were separated using 10% SDS-PAGE and stained with 0.5% Coomassie Brilliant Blue G-250 (AppliChem GmbH, Germany). The stained gel lanes were cut into 40 slices and subjected to in-gel tryptic digestion, as described in the Supplemental Materials and Methods.

Reverse-Phase LC–MS/MS and Protein Identification

For mass spectrometric (MS) protein identification, each in-gel digested peptide mixture was reconstituted in HPLC buffer A (0.1% formic acid; Sigma-Aldrich), loaded on to a trap column (Zorbax 300SB-C18, 0.3 × 5 mm; Agilent Technologies, Taiwan) at a flow rate of 0.2 μL/min in HPLC buffer A, and separated on a resolving 10 cm analytical C_{18} column (inner diameter, 75 μm) using a 15-μm tip (New Objective, Woburn, MA). The peptides were eluted using a linear gradient of 0–10% HPLC buffer B (99.9% ACN containing 0.1% formic acid) for 3 min, 10–30% buffer B for 35 min, 30–35% buffer B for 4 min, 35–50% buffer B for 1 min, 50–95% buffer B for 1 min, and 95% buffer B for 8 min, all at a flow rate of 0.25 μL/min across the analytical column.

The LC apparatus was coupled with a two-dimensional linear ion trap mass spectrometer (LTQ-Orbitrap, Thermo Fisher, CA, USA) operated using the Xcalibur 2.0 software package (Thermo Fisher). Intact peptides were detected in the Orbitrap at a resolution of 30000. Internal calibration was performed using the ion signal of $(Si(CH_3)_2O)_6H^+$ at m/z 445.120025 as a lock mass. For the MS analysis, we used a data-dependent procedure that alternated between one MS scan and six MS/MS scans for the six most abundant precursor ions. The m/z values selected for the MS/MS analyses were dynamically excluded for 180 s. The electrospray voltage was applied at 1.8 kV. Both MS and MS/MS spectra were acquired using the one microscan with maximum fill times of 1000 and 100 ms for the MS and MS/MS analyses, respectively. To prevent overfilling of the ion trap, automatic gain control was used. For the generation of MS/MS spectra, 5×10^4 ions were accumulated and resolved in the ion trap. For the MS scans, the m/z scan range was set at 350–2000 Da.

For database searching, the obtained MS/MS spectra were analyzed using the Mascot algorithm (Version 2.1, Matrix Science, Boston, MA) against the Swiss-Prot human sequence database (released Jun 15, 2010, selected for *Homo sapiens*, 20367 entries) of the European Bioinformatics Institute (EBI). The fragment ion mass tolerance was set to 0.5 Da and the parent ion mass tolerance was set to 10 ppm, with trypsin as the digestion enzyme. Up to one missed cleavage was allowed, and searches were performed with the parameters of: variable oxidation on methionine (+15.99 Da) and fixed carbamidomethylation on cysteine (+57 Da). A random sequence database was used to estimate false-positive rates for peptide matches.

After Mascot searching, the obtained files were processed through the Scaffold software (Version 3.1; Proteome Software, Portland, OR, USA). The Scaffold software includes the PeptideProphet,[23] which aids in the assignment of peptide MS spectra, as well as the ProteinProphet[24] program, which assigns and groups peptides to a unique protein/protein family when they are shared among several isoforms. We used PeptideProphet and ProteinProphet probabilities ≥0.95 to ensure an overall false-discovery rate below 0.5%. Only proteins with two or more identified peptides were retained in this study.

Bioinformatics

For relative quantification of proteins, we performed label-free comparison of the secretomes of primary OSCC cells (POC) and adjacent noncancerous cells (PANC), using spectral counting to ascertain dysregulated proteins. The numbers of spectra assigned for each protein were exported from the Scaffold software in the MS Excel format. The normalized spectral count (SC) of each protein in the experiment was obtained by dividing the SC of a given protein with the total SC of the experiment. The fold change was determined by dividing the average SC from POC by that from PANC. We failed to identify all proteins in all experiments; unidentified proteins or missing values in a particular sample were assigned a SC of one to avoid dividing by zero and to prevent overestimation of fold changes. Proteins with ratios below the mean of all ratios minus two standard deviations (SD) of all ratios were considered to be underexpressed, while those above the mean plus two SD were considered to be overexpressed.

The cell secretome were classified by principal component analysis and hierarchical clustering analysis, as applied by Partek Genomics Suites (Partek Inc., St. Louis, MO, USA) and described in detail in the Supplemental Materials and Methods. The DAVID classification system (http://david.abcc.ncifcrf.gov/) was used to test for enrichment of certain biological processes.[25,26] Any gene ontology (GO) biological process with a false-discovery rate (FDR) < 0.05 was considered to be significant in the enrichment analysis.

To predict the secretion pathways of the identified proteins, we used SignalP with Hidden Markov models to estimate the presence of secretory signal peptide sequences,[27] SecretomeP to deduce nonsignal peptide-triggered protein secretion,[28] and the transmembrane Hidden Markov model (TMHMM) to predict transmembrane helices.[29]

Immunohistochemistry and Scoring

Immunohistochemical (IHC) staining was performed on paraffin-embedded tissues using goat polyclonal anti-THBS2 (Santa Cruz Biotechnology, Dallas, TX, USA), rabbit polyclonal anti-UFD1L (ProteinTech, Chicago, IL, USA), and rabbit polyclonal anti-DNAJB11 (Abcam, Cambridge, MA, USA). The detailed procedures for IHC staining and scoring are described in the Supplemental Materials and Methods.

Bead-Based Immunoassay for Salivary THBS2 Detection

We previously established a bead-based immunoassay for determining the serum levels of proteins in cancer patients.[17,30] To determine the salivary concentration of THBS2, we used our previous work to develop a bead-based immunoassay for THBS2, as detailed in the Supplemental Materials and Methods.

Statistical Analysis

The correlations of SC between duplicates were evaluated by Pearson correlation. The between-group differences in target-protein IHC scores and saliva levels were evaluated using the Mann–Whitney *U* test. The associations of IHC scores with the clinicopathological characteristics of cancer patients were examined by the Wilcoxon rank-sum test. Survival rates were obtained using the Kaplan–Meier method and compared by

dx.doi.org/10.1021/pr500038k | J. Proteome Res. XXXX, XXX, XXX–XXX

the log-rank test. The receiver operator characteristic (ROC) curve was constructed by plotting the sensitivities for given specificity levels of THBS2, and then calculating the area under the curve (AUC). All analyses were performed using SPSS (version 20.0; IBM, Armonk, NY, USA). A p value <0.05 was considered statistically significant.

RESULTS

Secretome Profiling of Primary Cells Derived from OSCC and Adjacent Noncancerous Epithelium Tissues

Although profiling of the cancer cell secretome is a practical approach for discovering potential cancer biomarkers, questions remain regarding the selection of useful candidates from the growing list of identified proteins. Owing to the lack of secretome data from noncancerous epithelial cells corresponding to most solid tumor types, data from other omics-related analyses have been used to facilitate the isolation of biomarker candidates from cancer cell secretomes; these include data from cancer-related body fluid proteomes,[10−14] tissue transcriptomes,[16−18] and the Human Protein Atlas.[8,19] To profile the secretome of OSCC and the corresponding noncancerous epithelial cells, we established primary cell cultures from paired OSCC (POC) and adjacent noncancerous (PANC) tissues from three OSCC patients (Figure 1A and Table 1). As shown in Supplemental Figure S1, the primary cultured cells showed strong staining of cytokeratins but not the fibroblast marker, Thy-1, indicating that they were appropriately derived from oral epithelia.

Proteins were collected from 24-h serum-free conditioned media of these primary cultures (Figure 1A). Due to low protein yields from the two POC cultures (Table 1), the secreted proteins from these two cultures were pooled. Proteins were initially separated with SDS-PAGE and stained with Coomassie blue (Figure 1B). Cell extracts were simultaneously evaluated to confirm the enrichment of secreted proteins in conditioned media. The protein patterns clearly differed between the conditioned media and cell extracts, indicating that the proteins in conditioned media were not due to cell death. The gels were sliced into 40 fractions. Each gel slice was divided into two for technical duplicates, digested individually with trypsin, and then analyzed using LC−MS/MS. A spectral search was performed against the Swiss-Prot database using the Mascot algorithm, and the results were further analyzed using Scaffold software (Figure 1A). Based on cutoffs of peptide probability ≥0.95 and protein probability ≥0.95, we detected 1761 and 1741 proteins with ≥2 peptide hits in the conditioned media from POC and PANC, respectively (Supplemental Figure S2A and Table S1−S3). Among the proteins identified, 1419 and 1414 proteins were identified in both experiments for POC and PANC cells, respectively. The reproducibility of protein identification between the technical duplicates was 81% (Supplemental Figure S2A). To estimate the false-discovery rate (FDR) of our peptide identification, we additionally searched the spectra against a decoy database. All FDRs were <0.03% (Supplemental Table S1).

To compare the secretomes between primary cultured cells and cell lines, we analyzed the secretomes of four OSCC cell lines using the same criteria (Figure 1B). The conditioned media from SCC25, SAS, OEC-M1, and OC3 cells yielded 1581, 1517, 1402, and 1143 proteins, respectively (Supplemental Table S1 and S4), for a total of 2134 nonredundant proteins identified across the four cell lines (Figure 1C and Supplemental Table S5).

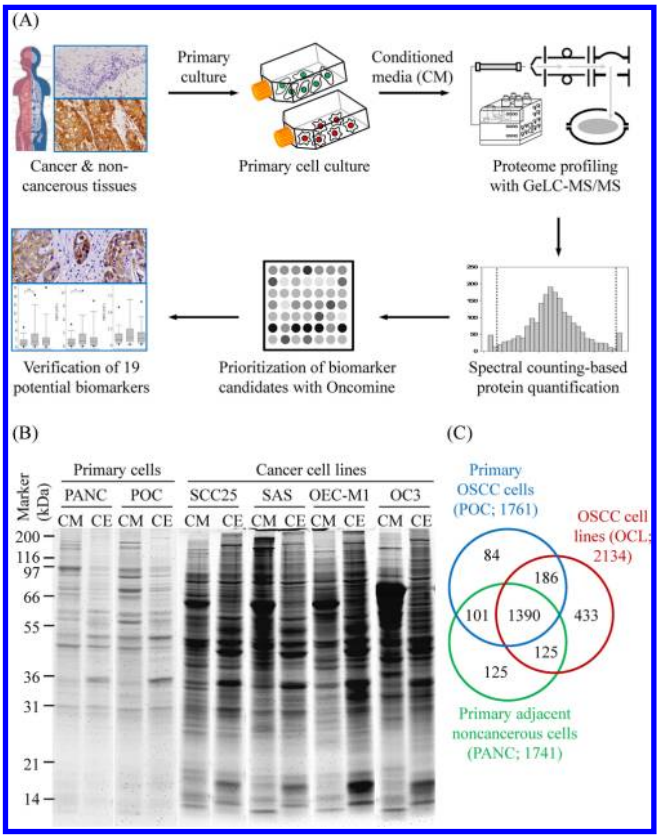

Figure 1. Identification of OSCC biomarker candidates via secretome profiling of primary cultured cells in conjunction with tissue transcriptome analysis. (A) The strategy consists of secretome profiling of primary cultured OSCC cells, label-free protein quantification, and OSCC tissue transcriptome analysis, followed by verification using clinical specimens. (B) Conditioned media (CM) and cell extracts (CE) from primary OSCC cells (POC), primary adjacent noncancerous cells (PANC), and OSCC cell lines (OCLs) were collected and processed as described in the Materials and Methods. Proteins (20 and 50 μg for primary cultured cells and cell lines, respectively) were separated by 10% SDS-PAGE and stained with Coomassie blue. (C) Venn diagrams show overlaps between the proteins identified in CM from POC, PANC, and OCLs. The total numbers of identified proteins are listed in brackets.

The proteins identified as being secreted by POC, PANC, and the cell lines were analyzed for overlapping members. Among 2444 nonredundant proteins, 1390 (56.87%) were found in all of the studied secretomes (Figure 1C and Supplemental Table S5), whereas 84 (3.44%), 125 (5.11%), and 433 (17.72%) proteins were uniquely detected in POC, PANC, and the cancer cell lines, respectively (Figure 1C and Supplemental Table S5). Notably, 186 (7.61%) proteins were found in the studied cancer cells (POC and the cancer cell lines) but not in the noncancerous cells, while 101 (4.13%) proteins were found in the primary cell cultures (POC and PANC) but not in the cell lines (Figure 1C and Supplemental Table S5).

Distribution and Ontology of the Identified Proteins

The secretory routes of the identified proteins were predicted based on their protein sequences (Supplemental Table S5). The SignalP program predicted that 389 and 334 proteins from POC and PANC, respectively, are released through the classical

dx.doi.org/10.1021/pr500038k | J. Proteome Res. XXXX, XXX, XXX−XXX

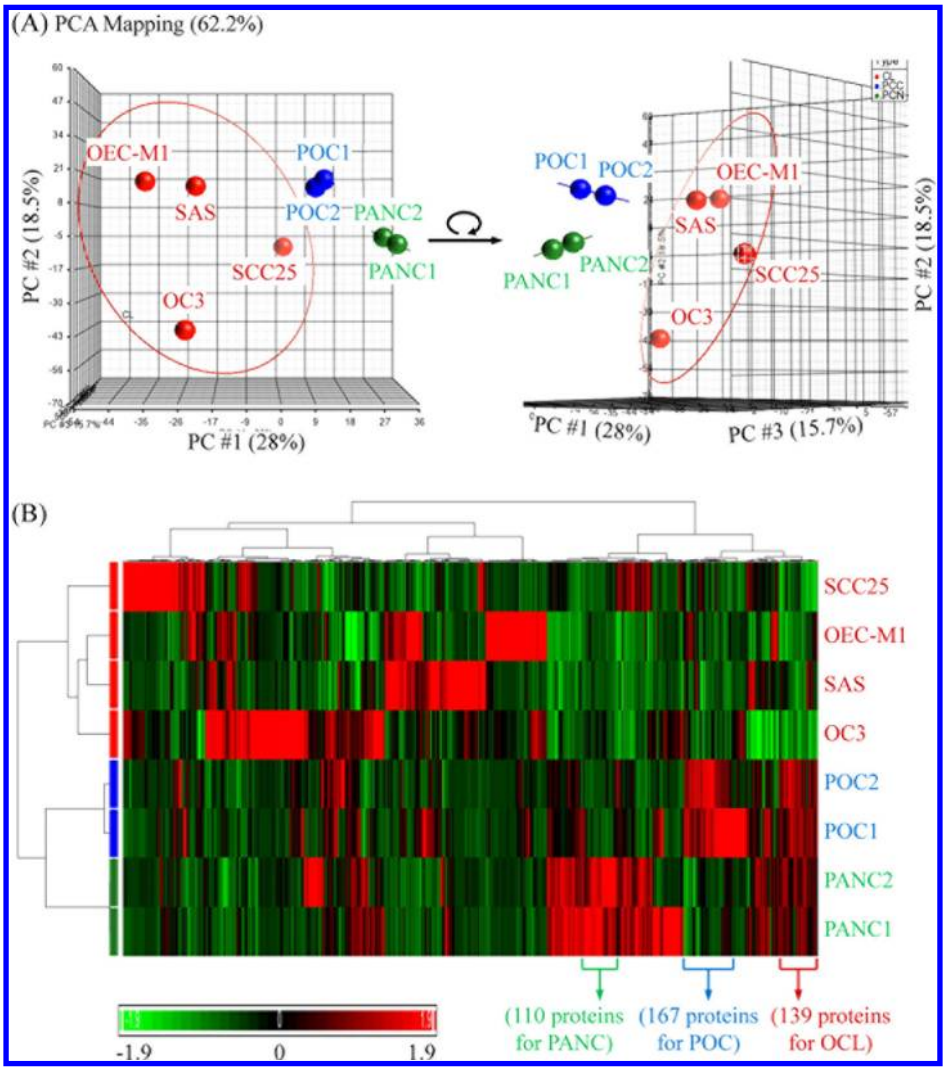

Figure 2. Principal component analysis and hierarchical clustering based on the cell secretome profiles was performed. The normalized spectral counts of all identified proteins were transformed to *Z* scores and analyzed via principal component analysis (PCA) and unsupervised hierarchical clustering (HCL). (A) Front view (left panel) and lateral view (right panel) of the PCA map for the first three eigenvectors. The numbers in parentheses represent the percent variation accounted for by each principal component. (B) Unsupervised two-way HCL was performed according to Pearson similarity and Ward's linkage method. Cells are shown in the rows, and proteins are shown in the columns. The numbers of proteins possessing unique features that could be used to sort the POC, PANC, and cancer cell lines are listed in brackets. The heat map scale of *Z* scores ranges from −1.9 (green) to 1.9 (red) with a midpoint of 0 (black).

secretion pathway (SignalP probability ≥0.9; Supplemental Table S6), while 583 and 589 proteins, respectively, were predicted to be secreted via the nonclassical secretion pathways (SignalP probability <0.9 and SecretomeP score ≥0.5; Supplemental Table S6). Among the proteins that could not be categorized into either secretion pathway, 36 from POC and 30 from PANC were predicted to have transmembrane helixes and thus could be released via membrane shedding (Supplemental Table S6). These results collectively predict that 57.2% (1008/1761) and 54.7% (953/1741) of the proteins identified from POC and PANC, respectively, could be released to the media via different mechanisms (Supplemental Table S6). Notably, the percentages of identified proteins that distributed to the different predicted secretory routes were similar in the primary cell cultures and cancer cell lines (Supplemental Table S6).

The identified proteins were then functionally classified based on their GO molecular functions and biological processes. Unexpectedly, the category rankings of the GO molecular functions and biological processes were nearly identical between the primary cell cultures and OSCC cell lines (Supplemental Figure S3).

Hierarchical Clustering Analysis of Proteins Secreted from Primary Cell Cultures and Cancer Cell Lines

In an effort to reveal potential pathways involved in the regulation of cancer microenvironments, we attempted to distinguish primary cells from cancer cell lines according to the abundance of their secreted proteins. Toward this end, we used the SC data to perform relative quantification of the identified proteins.[31] To minimize between-sample variations in protein quantity, the SC of each individual protein was divided by the total SC of the samples. As shown in Supplemental Figure S2B, the normalized SC showed significant correlations between duplicate experiments for secretome profiling of the primary cell cultures (r = 0.946 and 0.955 for POC and PANC, respectively), suggesting that normalized SC can be used to

dx.doi.org/10.1021/pr500038k | J. Proteome Res. XXXX, XXX, XXX−XXX

Table 2. List of 19 Biomarker Candidates Whose Genes Are Up-regulated in OSCC Tissues As Compared with Noncancerous Tissues

			gene expression ratio (p value) in transcriptome data sets[b]					
gene symbol	protein name (Swiss-Prot accn no.)	$\log_2$ ratio of POC/PANC[a]	Ginos head-neck	Peng head-neck	Estilo head-neck	Pyeon multicancer	Talbot lung	Ye head-neck
DKK1[c]	Dickkopf-related protein 1 (DKK1_HUMAN)[c]	6.35	2.36 (<0.001)	3.73 (<0.001)	3.11 (0.001)	1.98 (0.025)	1.55 (0.003)	1.41 (0.135)
VEGFC[c,d]	Vascular endothelial growth factor C (VEGFC_HUMAN)[c,d]	6.00	2.06 (<0.001)	2.82 (<0.001)	4.40 (<0.001)	3.14 (<0.001)	1.51 (0.001)	2.34 (0.003)
ATP1A1	Sodium/potassium-transporting ATPase subunit α1 (AT1A1_HUMAN)	5.61	1.61 (<0.001)	1.36 (<0.001)	N/A	2.11 (<0.001)	N/A	1.52 (0.017)
LCP1	Plastin-2 (PLSL_HUMAN)	4.95	2.19 (<0.001)	1.79 (<0.001)	2.38 (<0.001)	1.08 (0.225)	1.63 (0.007)	1.04 (0.283)
NT5E[d]	5′-nucleotidase (5NTD_HUMAN)[d]	4.88	2.72 (<0.001)	4.15 (<0.001)	3.28 (<0.001)	3.48 (<0.001)	1.69 (<0.001)	1.58 (0.003)
LOXL2	Lysyl oxidase homologue 2 (LOXL2_HUMAN)	4.67	3.68 (<0.001)	1.98 (<0.001)	3.47 (<0.001)	2.13 (<0.001)	1.78 (<0.001)	2.65 (<0.001)
LUM	Lumican (LUM_HUMAN)	4.44	3.11 (<0.001)	1.50 (0.029)	2.43 (<0.001)	6.12 (<0.001)	2.03 (<0.001)	2.41 (0.004)
RAP1B[c]	Ras-related protein Rap-1b (RAP1B_HUMAN)[c]	4.23	2.01 (<0.001)	3.48 (<0.001)	2.23 (<0.001)	1.96 (<0.001)	2.18 (<0.001)	1.56 (0.006)
COL5A1	Collagen alpha-1(V) chain (CO5A1_HUMAN)	4.15	4.78 (<0.001)	1.54 (<0.001)	N/A	3.03 (<0.001)	N/A	2.70 (0.002)
UFD1L[d]	Ubiquitin fusion degradation protein 1 homologue (UFD1_HUMAN)[d]	4.10	1.18 (0.026)	1.71 (<0.001)	2.15 (<0.001)	1.75 (<0.001)	1.86 (<0.001)	1.52 (<0.001)
CFB	Complement factor B (CFAB_HUMAN)	4.04	3.01 (<0.001)	2.27 (<0.001)	3.14 (<0.001)	3.30 (<0.001)	1.68 (<0.001)	1.79 (0.010)
DNAJB11[d]	DnaJ homologue subfamily B member 11 (DJB11_HUMAN)[d]	3.97	N/A	1.55 (<0.001)	N/A	3.02 (<0.001)	N/A	1.79 (<0.001)
HLA-C	HLA class I histocompatibility antigen, Cw-12α chain (1C12_HUMAN)	3.90	2.25 (<0.001)	2.11 (<0.001)	N/A	2.41 (<0.001)	N/A	1.45 (0.002)
GOLM1	Golgi membrane protein 1 (GOLM1_HUMAN)	3.80	11.12 (<0.001)	2.09 (<0.001)	N/A	1.88 (0.002)	N/A	1.05 (0.049)
THBS2	Thrombospondin-2 (TSP2_HUMAN)	3.64	2.77 (<0.001)	2.14 (<0.001)	3.58 (<0.001)	2.33 (0.001)	2.67 (<0.001)	1.67 (0.052)
FN1[c]	Fibronectin (FINC_HUMAN)[c]	3.56	5.80 (<0.001)	4.83 (<0.001)	3.03 (<0.001)	8.21 (<0.001)	2.33 (<0.001)	2.09 (0.034)
C1S	Complement C 1s subcomponent (C1S_HUMAN)	3.50	1.55 (<0.001)	1.47 (0.005)	1.78 (<0.001)	3.15 (<0.001)	1.66 (<0.001)	−1.08 (0.603)
SFRS3	Splicing factor, arginine/serine-rich 3 (SFRS3_HUMAN)	3.48	1.31 (0.007)	1.10 (0.182)	2.09 (<0.001)	1.97 (0.001)	1.98 (<0.001)	1.64 (<0.001)
F3[c]	Tissue factor (TF_HUMAN)[c]	3.42	−1.61 (0.979)	1.56 (<0.001)	3.93 (<0.001)	1.42 (0.072)	3.41 (<0.001)	1.77 (0.012)

[a]The values represent the $\log_2$ POC/PANC ratio of normalized spectral counts in the secretome profiling. [b]The gene expression information on six transcriptome data sets was taken from the Oncomine 4.4 Research Edition. The expression ratios were shown as tumor versus normal tissues. The Ginos data set (ref 32): comparison between head and neck cancer and normal tissues. The Peng data set (ref 33): comparison between oral squamous cell carcinoma and normal tissues. The Estilo (ref 34), Pyeon (ref 35), Talbot (ref 36), and Ye (ref 37) data sets: comparison between tongue squamous cell carcinoma and normal tissues. [c]The expression of protein has been previously reported to be dysregulated in OSCC tissues. [d]The candidate is one of the 167 proteins with the most different features used to distinguish the POC from cell lines and PANC (Figure 2B).

dx.doi.org/10.1021/pr500038k | J. Proteome Res. XXXX, XXX, XXX−XXX

estimate the relative abundance of proteins in conditioned media.

To perform principal component analysis (PCA) and unsupervised hierarchical clustering (HCL) analysis, each normalized SC was then transformed to a *Z* score. As shown in Figure 2, our PCA and HCL analyses could clearly differentiate between the secretome profiles of primary cultured cells and the OSCC cell lines. Notably, both analyses could also discriminate between the secretome profiles of POC and PANC (Figure 2). We further selected 167, 110, and 139 proteins with the most different features used to distinguish POC, PANC, and the cell lines, respectively (Figure 2B and Supplemental Table S7). To clarify the potential biological processes involved, DAVID (v6.7) was used to analyze the secreted proteins for enrichment of GO categories. As shown in Supplemental Figure S4, the proteins that could be used to distinguish POC were highly correlated with protein folding, and those that could distinguish the OSCC cell lines were highly correlated with protein transport, protein localization, and cell redox homeostasis. In contrast, no biological process was significantly enriched among the proteins that could be used to distinguish PANC. Collectively, these results demonstrate that OSCC primary cell cultures are distinct from OSCC cell lines in terms of the secreted protein levels and their involved biological networks.

Spectral Counting-Based Quantification for Discovery of OSCC Biomarkers

To identify OSCC biomarker candidates, the relative levels of 2011 proteins released by the primary cultured cells were estimated by spectral counting-based quantification (Figure 1A and Supplemental Table S8). The fold change of each protein was determined by dividing the average SC of the protein in POC by that in PANC. Proteins with ratios less than the mean ratio minus two SD of all ratios ($\log_2$ POC/PANC ratio < −3.205) were considered to be underexpressed, while those with ratios above the mean plus two SD ($\log_2$ POC/PANC ratio > 3.246) were considered overexpressed. On this basis, we found that the levels of 64 and 51 proteins were significantly elevated and decreased, respectively, in POC versus PANC (Supplemental Figure S5 and Table S8).

To efficiently isolate potential OSCC markers from the 64 elevated proteins, we used the Oncomine 4.4 database, which contains several oral cancer tissue-related microarray data sets, and examined the expression levels of the 64 proteins in cancerous and noncancerous oral tissues (Figure 1A). Six OSCC-related data sets were examined (Supplemental Table S9): one comparing head-and-neck squamous cell carcinoma with control tissues,[32] one for oral cavity carcinoma versus normal tissues,[33] and four for tongue squamous cell carcinoma versus normal tissues.[34−37] Compared with noncancerous tissues, 19 of the 64 proteins were found to be overexpressed in cancer tissues (>1.5-fold, $p < 0.05$ cutoff) in over half of the evaluated data sets (Table 2 and Supplemental Table S10). Among the 19 proteins, Dickkopf-related protein 1, vascular endothelial growth factor C, fibronectin, and tissue factor were previously reported to be up-regulated in OSCC tissues (Table 2),[38−41] while the Ras-related protein Rap-1b was previously suggested to play a role in the malignant process of oral cancer cells.[42] Therefore, although it is perhaps arbitrary to select biomarker candidates on the basis of gene expression alone, the use of transcriptome analysis to narrow the 64 proteins to 19 candidate markers seems appropriate here.

Validation of THBS2, UFD1L, and DNAJB11 Overexpression in OSCC Tissues

Three candidates, thrombospondin-2 (THBS2), ubiquitin fusion degradation protein 1 homologue (UFD1L), and DnaJ homologue subfamily B member 11 (DNAJB11), were selected for further verification as OSCC biomarkers. To confirm that the levels of the three candidates are elevated in OSCC, immunohistochemical (IHC) analysis was used to examine their expression levels in tissue sections from OSCC patients. All three candidate markers were highly expressed in the cytoplasm of OSCC cells, whereas the paired pericancerous normal epithelia showed little or no expression of these proteins (Figure 3A). Compared to adjacent normal epithelia, the IHC scores for THBS2, UFD1L, and DNAJB11 were significantly higher in OSCC tissues (Figure 3B).

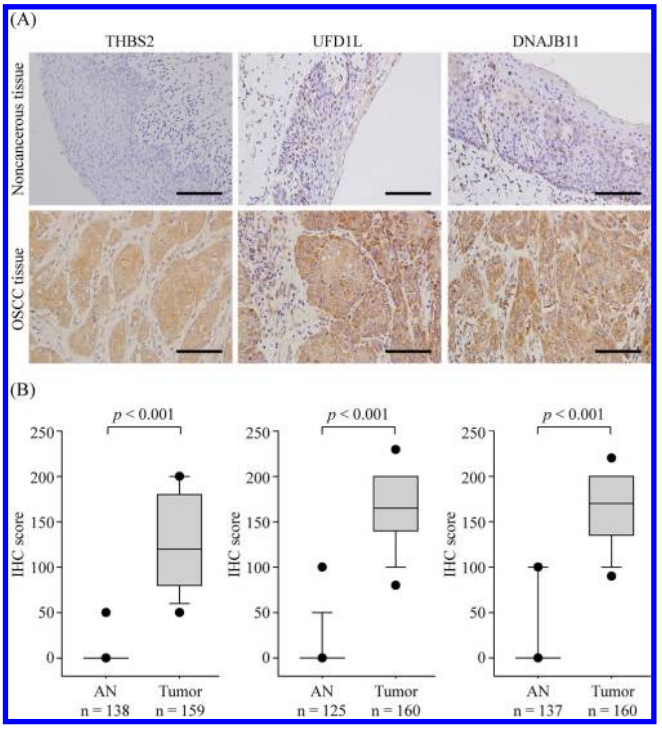

Figure 3. Elevated expression of THBS2, UFD1L, and DNAJB11 in OSCC tissues. (A) Immunohistochemical (IHC) staining of THBS2 (left panel), UFD1L (middle panel), and DNAJB11 (right panel) in paired adjacent noncancerous (upper panel) and OSCC (lower panel) tissues. Scale bar, 100 μm. Original magnification, ×400. (B) Box-plot analysis of the IHC scores obtained from paired adjacent noncancerous (AN) and tumor tissues. Data are presented as the upper and lower quartiles (box), the median value (horizontal lines), the middle 80% distribution (dashed line), and the middle 90% distribution (filled circles) of the IHC scores.

Next, we investigated whether the tissue levels of the three candidates were associated with the clinical manifestations of OSCC in these patients. Our analysis revealed that the levels of THBS2 and DNAJB11 in OSCC tissues were significantly elevated in patients with lymph node metastasis and positive perineural invasion (Table 3). Moreover, higher levels of THBS2 in OSCC tissues were correlated with larger size, advanced overall stage, and depth of the OSCC (Table 3). In contrast, there was no apparent correlation between UFD1L expression and patient age, pT status, pN status, overall

dx.doi.org/10.1021/pr500038k | J. Proteome Res. XXXX, XXX, XXX−XXX

Table 3. Correlation between Clinicopathological Features and the Tissue Levels of THBS2, UFD1L, and DNAJB11 in Untreated OSCC Patients

	THBS2		UFD1L		DNAJB11	
characteristic	IHC score[a]	p value[b]	IHC score[a]	p value[b]	IHC score[a]	p value[b]
gender						
female	113 ± 62 (21)	0.303	173 ± 59 (21)	0.070	167 ± 52 (21)	0.588
male	128 ± 54 (138)		160 ± 45 (139)		166 ± 43 (139)	
age (years)						
<49.9	132 ± 56 (80)	0.329	156 ± 48 (80)	0.096	159 ± 43 (80)	0.016
≥49.9	121 ± 54 (79)		168 ± 45 (80)		173 ± 45 (80)	
pT status						
T1-T2	117 ± 55 (84)	0.013	166 ± 47 (85)	0.078	171 ± 47 (85)	0.074
T3-T4	136 ± 54 (75)		157 ± 47 (75)		160 ± 41 (75)	
pN status						
pN negative	118 ± 53 (102)	0.006	158 ± 48 (105)	0.212	159 ± 46 (105)	0.005
pN positive	141 ± 56 (57)		169 ± 44 (55)		179 ± 39 (55)	
overall pathological stage						
I–II	111 ± 53 (62)	0.002	160 ± 49 (62)	0.940	168 ± 49 (62)	0.649
III–IV	136 ± 54 (97)		163 ± 45 (98)		165 ± 42 (98)	
cell differentiation[c]						
W-D and M-D	125 ± 55 (145)	0.608	162 ± 46 (147)	0.661	166 ± 45 (147)	0.558
P-D	135 ± 57 (14)		164 ± 51 (13)		172 ± 40 (13)	
perineural invasion						
no	116 ± 54 (109)	<0.001	158 ± 48 (114)	0.125	160 ± 47 (114)	0.007
yes	151 ± 49 (49)		172 ± 41 (45)		182 ± 31 (45)	
tumor depth						
≤8 mm	118 ± 55 (85)	0.016	166 ± 46 (86)	0.152	168 ± 47 (86)	0.665
>8 mm	137 ± 53 (73)		158 ± 46 (73)		165 ± 41 (73)	

[a]Data are shown as mean ± SD (case no.). [b]The p values between two groups were determined by the Mann–Whitney U test. [c]W-D, well-differentiation; M-D, moderate differentiation; P-D, poor differentiation.

pathological stage, cell differentiation, perineural invasion, or tumor depth (Table 3).

The prognostic values of the three candidate proteins with respect to OSCC patient survival were compared for patients with high and low protein levels (stratified using the median IHC score as the cutoff value). As shown by Kaplan–Meier plots, the long-term overall survival rates for patients with low and high tissue levels of THBS2 were 59.8% and 41.2%, respectively; this difference was statistically significant by log-rank test (p = 0.044; Figure 4A). A high tumor THBS2 protein level was also a significant prognostic factor for poor disease-free survival in OSCC patients. Compared to patients with low THBS2 levels in their tumor tissues, those with high cancer THBS2 levels had a significantly lower rate of long-term disease-free survival (58.3% versus 35.8%, p = 0.020; Figure 4B). However, our survival analyses did not demonstrate any significant difference when the patients were stratified by their tissue levels of UFD1L or DNAJB11.

Saliva Levels of THBS2 Are Elevated in OSCC Patients

To evaluate the three candidates as potential salivary biomarkers for OSCC, we examined their levels in saliva samples from healthy controls (n = 47), OSCC patients (n = 49), and noncancerous patients with oral potentially malignant disorder (OPMD; n = 47). The latter group was used to evaluate whether chronic inflammatory disease in the oral cavity could elevate the salivary levels of one or more of the candidate proteins. We measured salivary UFD1L levels using an in-house-developed ELISA and determined salivary THBS2 levels using a bead-based immunoassay. We were unable to measure the salivary levels of DNAJB11, as our attempts to establish an

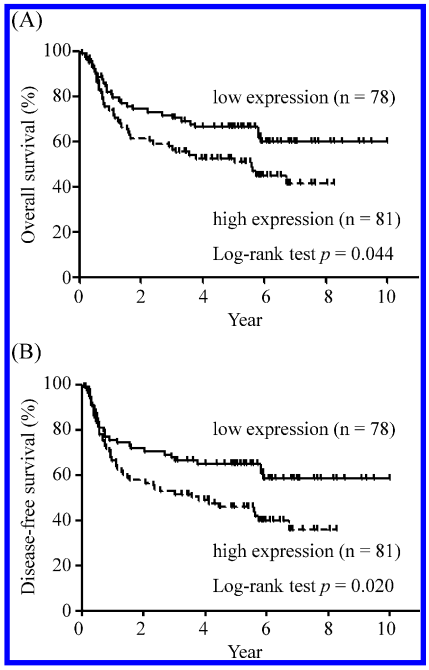

Figure 4. Elevated THBS2 levels in OSCC tissues are correlated with poor long-term survival of OSCC patients. (A) Kaplan–Meier plot showing that the long-term overall survival rates for patient subgroups stratified by THBS2 overexpression are 59.8% versus 41.2% (p = 0.044). (B) Kaplan–Meier plot showing that the long-term disease-specific survival rates for patient subgroups stratified by THBS2 overexpression are 58.3% versus 35.8% (p = 0.020).

dx.doi.org/10.1021/pr500038k | J. Proteome Res. XXXX, XXX, XXX–XXX

immunoassay were unsuccessful. As shown in Figure 5A, the salivary levels of THBS2 were significantly elevated in OSCC

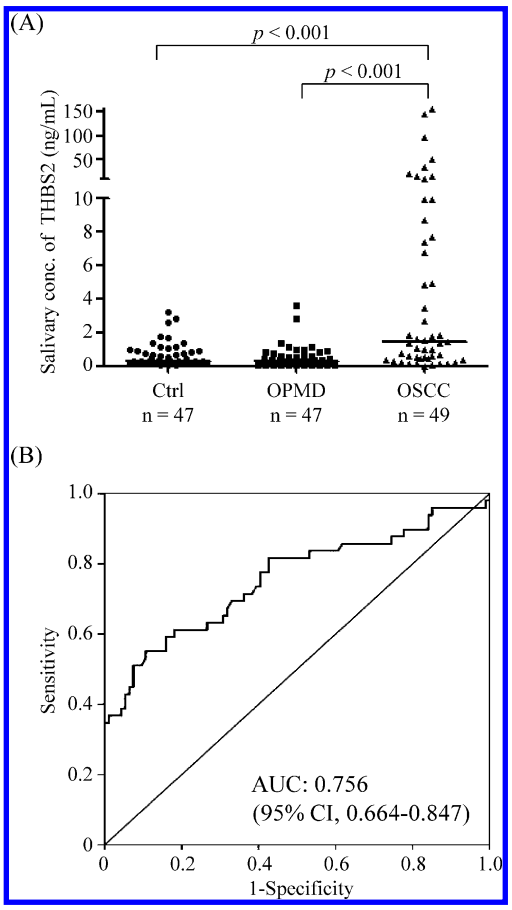

Figure 5. Saliva levels of THBS2 in OSCC patients. (A) A bead-based assay was used to measure salivary THBS2 levels in 47 healthy controls (Ctrl), 47 noncancerous individuals with oral potentially malignant disorder (OPMD), and 49 OSCC patients (OSCC). The horizontal lines indicate the median values. (B) ROC curve analysis for the use of THBS2 in discriminating between OSCC patients (n = 49) and non-OSCC individuals (healthy controls and OPMD individuals; n = 94).

patients compared to healthy controls (12.90 ± 32.81 versus 0.68 ± 0.73 ng/mL, $p < 0.001$) and OPMD individuals (12.90 ± 32.81 versus 0.51 ± 0.68 ng/mL, $p < 0.001$). In contrast, the salivary levels of UFD1L did not significantly differ between OSCC patients and healthy controls (data not shown).

The utility of THBS2 as an OSCC detection marker was further evaluated by receiver operating characteristic (ROC) curve analysis. For discriminating OSCC patients from non-OSCC individuals (healthy and OPMD individuals), the area under ROC curve (AUC) of THBS2 was determined as 0.756 (95% confidence interval, 0.664−0.847; Figure 5B). Using a cutoff value of 1.26 ng/mL for salivary THBS2, we found that the sensitivity and specificity values for OSCC detection were 55.1% and 89.4%, respectively.

DISCUSSION

To date, OSCC screening has relied on otolaryngologists or dentists performing visual inspections of the oral cavity, searching for possible signs of the disease. Despite an urgent need for biomarkers capable of improving OSCC screening, no candidate markers have yet been sanctioned for clinical use. This is largely due to the unsatisfying effectiveness of the studied molecules and/or a lack of rigorous validation in large cohort studies. Profiling of cancer cell secretomes has been proposed as a feasible strategy for discovering useful cancer biomarker candidates that are more likely to be detected in body fluids. Here, we simultaneously profile the secretomes of primary cells derived from OSCC and adjacent noncancerous epithelial tissues, in an attempt to identify novel OSCC biomarkers (Figure 1A). Although the secretomes of OSCC cell lines have been previously reported,[20,43] this is the first secretomic comparison between OSCC cell lines and primary OSCC cells, as well as between primary pericancerous normal epithelial and OSCC cells.

To put our secretome data into a biological context, we examined the identified proteins using spectral counting-based label-free quantification and hierarchical clustering analyses (Figure 2 and Supplemental Figure S4). Our data revealed that the primary cultured cells could be discriminated from the OSCC cell lines based on the abundances of certain secreted proteins (Figure 2 and Supplemental Table S7). More importantly, our pathway analysis suggested that protein transport, protein localization, and cell redox homeostasis were among the most differentially regulated biological processes in the OSCC cell lines compared to the primary cultured cells (Supplemental Figure S4B). In contrast, protein folding represented the most dysregulated biological process in the primary OSCC cells (Supplemental Figure S4A). Glucose-regulated protein 78 (GRP78), one of the proteins with unique feature used to distinguish POC from the other cells (Figure 2B and Supplemental Table S7), was previously reported to play a pivotal role in protein folding by triggering the unfolded protein response in cells under stress conditions, such as hypoxia and nutrient limitation.[44,45] A recent study found that GRP78 is overexpressed in OSCC tissues and correlated with oral cancer progression.[46] Here, we report for the first time that the levels of UFD1L and DNAJB11 (Table 2), two protein folding-related molecules,[47,48] were also significantly elevated in OSCC tissues compared to pericancerous normal epithelia (Figure 3). Collectively, our results indicate that secretome analysis of primary cultured cells may help us understand the behavior and microenvironment of OSCC *in vivo*.[49,50]

Since OSCC is immersed in saliva, the use of salivary markers for OSCC detection seems to be more effective than the use of serum markers.[51,52] Here, we found that the salivary levels of THBS2 are significantly elevated in OSCC patients compared to healthy controls (Figure 5A), whereas serum THBS2 levels did not significantly differ between 133 OSCC patients and 146 healthy individuals (14.2 ± 10.9 versus 14.3 ± 9.0 ng/mL, p = 0.243; data not shown). Notably, the salivary levels of THBS2 were not elevated in the OPMD patients (Figure 5A), indicating that the increase in salivary THBS2 observed in the OSCC group was not due to chronic inflammation of the oral cavity. As saliva specimens may be readily and non-invasively collected in clinical practice, our results suggest that salivary THBS2 could potentially be used as an OSCC biomarker, perhaps in combination with visual oral examination to improve OSCC screening. Recently, the salivary levels of the IL8 protein and the SAT mRNA were reported to be capable of discriminating OSCC patients from healthy subjects.[53] To improve OSCC diagnosis, future studies are warranted to evaluate the detection efficacy of a combined panel of the salivary proteins (THBS2 and IL8) and the SAT mRNA with the same cohorts.

dx.doi.org/10.1021/pr500038k | J. Proteome Res. XXXX, XXX, XXX−XXX

ELISA is currently the most commonly used method for validating biomarker candidates in body fluids, as its high specificity and sensitivity allow proteins to be measured at plasma/serum concentrations in the range of low ng/mL to pg/mL. However, the commercially available immunoassays are generally expensive, and it can be time-consuming to establish new immunoassays. The need for specific antibodies against candidate proteins and the time required to develop new immunoassays typically create bottlenecks in biomarker validation.[54] Multiple reaction monitoring-mass spectrometry (MRM-MS) is now being used as an effective tool for accurately quantifying candidate proteins without the need for specific antibodies. Dozens of marker candidates can be quantified in a single LC-MRM-MS run, which detects Q1/Q3 ion pairs of signature peptides that are representatives of marker candidates.[54,55] In the future, this technique could be used to validate the identified OSCC marker candidates, especially those for which ELISA is not feasible.

THBS2 is an adhesive matricellular glycoprotein that participates in the modulation of cell-matrix interactions.[56,57] Several previous studies have demonstrated that it plays a role in inhibiting tumor growth and angiogenesis,[58−60] but its expression profile in cancers remains controversial. THBS2 is reportedly down-regulated in cervical cancer,[59] non-small cell lung cancer,[61] and ovarian cancer,[62] whereas it is reportedly overexpressed in pulmonary adenocarcinoma,[58] multiple myeloma,[63] and colorectal cancer.[64] Recently, Reis et al. used a meta-analysis of 199 samples (OSCC and normal oral tissues) from five public microarray data sets plus an in-house microarray analysis using 96 tissue samples from 24 OSCC patients to identify a gene signature for OSCC recurrence.[65] They identified a four-gene signature (MMP1, COL4A1, P4HA2, and THBS2) that had value for OSCC prognosis, and used quantitative real-time PCR to confirm that the THBS2 gene is overexpressed in OSCC tissues.[65] Consistent with this recent finding, we herein show for the first time that THBS2 protein levels are significantly elevated in OSCC tissues compared to pericancerous normal epithelia (Figure 3). Importantly, we further report that elevated levels of THBS2 in cancer tissues are associated with positive lymph node metastasis, perineural invasion and poorer patient survival (Figure 4 and Table 3).

In conclusion, we herein profiled the secretomes of primary cells derived from OSCC and pericancerous normal epithelial tissues. The differentially expressed proteins and dysregulated biological processes exhibited by primary OSCC cells were revealed by spectral counting-based protein quantification and hierarchical clustering. To the best of our knowledge, this study is one of the few in which proteomic discovery has been integrated with data-mining bioinformatics to assess the secretome of primary cells and prioritize candidates for further marker evaluation. Among the isolated marker candidates, THBS2 was confirmed as a potential salivary marker for OSCC detection, and elevated levels of THBS2 in OSCC tissues were associated with worsened OSCC outcome. These results indicate that secretome profiling of primary cells is a feasible strategy for biomarker discovery, and that THBS2 may prove useful as a salivary biomarker for OSCC.

■ ASSOCIATED CONTENT

Supporting Information

Supplemental tables and figures as described in the text. This material is available free of charge via the Internet at http://pubs.acs.org.

■ AUTHOR INFORMATION

Corresponding Authors

*Phone: 886-3-2118800, ext. 5645. Fax: 886-3-2118891. E-mail: dr.kpchang@gmail.com.
*Phone: 886-3-2118800, ext. 5093. Fax: 886-3-2118800, ext. 5497. E-mail: luckywu@mail.cgu.edu.tw.

Author Contributions

¶These authors contributed equally to this work.

Notes

The authors declare no competing financial interest.

■ ACKNOWLEDGMENTS

This work was supported by grants to Chang Gung University from the Ministry of Education, Taiwan (EMRPD1C0021); grants to C.-C.W. from the Ministry of Science and Technology (MOST), Taiwan (102-2325-B-182-014 and 102-2320-B-182-029-MY3); grants to K.-P.C. from the MOST (99-2320-B-182A-017-MY3 and 102-2628-B-182-015-MY3) and Chang Gung Memorial Hospital (CMRPG3D0261 and CMRPG1B0551), Taiwan; and grants to J.-S.Y. from the MOST (102-2325-B-182-010), the Health Promotion Administration, Ministry of Health and Welfare (PMRPD1B0102), and the Chang Gung Memorial Hospital (CLRPD190012 and 190013), Taiwan.

■ REFERENCES

(1) Siegel, R.; Naishadham, D.; Jemal, A. Cancer statistics, 2013. *CA Cancer J. Clin.* **2013**, *63* (1), 11−30.
(2) Mashberg, A. Comment on Head and neck cancer. *N. Engl. J. Med.* **1993**, *328* (24), 1783. Author reply 1784.
(3) Chen, Y. J.; Chang, J. T.; Liao, C. T.; Wang, H. M.; Yen, T. C.; Chiu, C. C.; Lu, Y. C.; Li, H. F.; Cheng, A. J. Head and neck cancer in the betel quid chewing area: recent advances in molecular carcinogenesis. *Cancer Sci.* **2008**, *99* (8), 1507−14.
(4) Mashberg, A. Diagnosis of early oral and oropharyngeal squamous carcinoma: obstacles and their amelioration. *Oral Oncol.* **2000**, *36* (3), 253−5.
(5) Kulasingam, V.; Diamandis, E. P. Strategies for discovering novel cancer biomarkers through utilization of emerging technologies. *Nat. Clin. Pract. Oncol.* **2008**, *5* (10), 588−99.
(6) Lin, Q.; Tan, H. T.; Lim, H. S.; Chung, M. C. Sieving through the cancer secretome. *Biochim. Biophys. Acta* **2013**, *1834* (11), 2360−71.
(7) Pavlou, M. P.; Diamandis, E. P. The cancer cell secretome: a good source for discovering biomarkers? *J. Proteomics* **2010**, *73* (10), 1896−906.
(8) Wu, C. C.; Hsu, C. W.; Chen, C. D.; Yu, C. J.; Chang, K. P.; Tai, D. I.; Liu, H. P.; Su, W. H.; Chang, Y. S.; Yu, J. S. Candidate serological biomarkers for cancer identified from the secretomes of 23 cancer cell lines and the human protein atlas. *Mol. Cell. Proteomics* **2010**, *9* (6), 1100−17.
(9) Loei, H.; Tan, H. T.; Lim, T. K.; Lim, K. H.; So, J. B.; Yeoh, K. G.; Chung, M. C. Mining the gastric cancer secretome: identification of GRN as a potential diagnostic marker for early gastric cancer. *J. Proteome Res.* **2012**, *11* (3), 1759−72.
(10) Planque, C.; Kulasingam, V.; Smith, C. R.; Reckamp, K.; Goodglick, L.; Diamandis, E. P. Identification of five candidate lung cancer biomarkers by proteomics analysis of conditioned media of four lung cancer cell lines. *Mol. Cell. Proteomics* **2009**, *8* (12), 2746−58.

(11) Wang, C. L.; Wang, C. I.; Liao, P. C.; Chen, C. D.; Liang, Y.; Chuang, W. Y.; Tsai, Y. H.; Chen, H. C.; Chang, Y. S.; Yu, J. S.; Wu, C. C.; Yu, C. J. Discovery of retinoblastoma-associated binding protein 46 as a novel prognostic marker for distant metastasis in nonsmall cell lung cancer by combined analysis of cancer cell secretome and pleural effusion proteome. *J. Proteome Res.* **2009**, *8* (10), 4428−40.

(12) Faca, V. M.; Ventura, A. P.; Fitzgibbon, M. P.; Pereira-Faca, S. R.; Pitteri, S. J.; Green, A. E.; Ireton, R. C.; Zhang, Q.; Wang, H.; O'Briant, K. C.; Drescher, C. W.; Schummer, M.; McIntosh, M. W.; Knudsen, B. S.; Hanash, S. M. Proteomic analysis of ovarian cancer cells reveals dynamic processes of protein secretion and shedding of extra-cellular domains. *PLoS One* **2008**, *3* (6), e2425.

(13) Gunawardana, C. G.; Kuk, C.; Smith, C. R.; Batruch, I.; Soosaipillai, A.; Diamandis, E. P. Comprehensive analysis of conditioned media from ovarian cancer cell lines identifies novel candidate markers of epithelial ovarian cancer. *J. Proteome Res.* **2009**, *8* (10), 4705−13.

(14) Bernhard, O. K.; Greening, D. W.; Barnes, T. W.; Ji, H.; Simpson, R. J. Detection of cadherin-17 in human colon cancer LIM1215 cell secretome and tumour xenograft-derived interstitial fluid and plasma. *Biochim. Biophys. Acta* **2013**, *1834* (11), 2372−9.

(15) Wu, C. C.; Chen, H. C.; Chen, S. J.; Liu, H. P.; Hsieh, Y. Y.; Yu, C. J.; Tang, R.; Hsieh, L. L.; Yu, J. S.; Chang, Y. S. Identification of collapsin response mediator protein-2 as a potential marker of colorectal carcinoma by comparative analysis of cancer cell secretomes. *Proteomics* **2008**, *8* (2), 316−32.

(16) Pavlou, M. P.; Dimitromanolakis, A.; Diamandis, E. P. Coupling proteomics and transcriptomics in the quest of subtype-specific proteins in breast cancer. *Proteomics* **2013**, *13* (7), 1083−95.

(17) Chang, Y. T.; Wu, C. C.; Shyr, Y. M.; Chen, T. C.; Hwang, T. L.; Yeh, T. S.; Chang, K. P.; Liu, H. P.; Liu, Y. L.; Tsai, M. H.; Chang, Y. S.; Yu, J. S. Secretome-based identification of ULBP2 as a novel serum marker for pancreatic cancer detection. *PLoS One* **2011**, *6* (5), e20029.

(18) Chang, K. P.; Wu, C. C.; Chen, H. C.; Chen, S. J.; Peng, P. H.; Tsang, N. M.; Lee, L. Y.; Liu, S. C.; Liang, Y.; Lee, Y. S.; Hao, S. P.; Chang, Y. S.; Yu, J. S. Identification of candidate nasopharyngeal carcinoma serum biomarkers by cancer cell secretome and tissue transcriptome analysis: potential usage of cystatin A for predicting nodal stage and poor prognosis. *Proteomics* **2010**, *10* (14), 2644−60.

(19) Sepiashvili, L.; Hui, A.; Ignatchenko, V.; Shi, W.; Su, S.; Xu, W.; Huang, S. H.; O'Sullivan, B.; Waldron, J.; Irish, J. C.; Perez-Ordonez, B.; Liu, F. F.; Kislinger, T. Potentially novel candidate biomarkers for head and neck squamous cell carcinoma identified using an integrated cell line-based discovery strategy. *Mol. Cell. Proteomics* **2012**, *11* (11), 1404−15.

(20) Yu, C. J.; Chang, K. P.; Chang, Y. J.; Hsu, C. W.; Liang, Y.; Yu, J. S.; Chi, L. M.; Chang, Y. S.; Wu, C. C. Identification of guanylate-binding protein 1 as a potential oral cancer marker involved in cell invasion using omics-based analysis. *J. Proteome Res.* **2011**, *10* (8), 3778−88.

(21) Pan, C.; Kumar, C.; Bohl, S.; Klingmueller, U.; Mann, M. Comparative proteomic phenotyping of cell lines and primary cells to assess preservation of cell type-specific functions. *Mol. Cell. Proteomics* **2009**, *8* (3), 443−50.

(22) Sandberg, R.; Ernberg, I. The molecular portrait of in vitro growth by meta-analysis of gene-expression profiles. *Genome Biol.* **2005**, *6* (8), R65.

(23) Keller, A.; Nesvizhskii, A. I.; Kolker, E.; Aebersold, R. Empirical statistical model to estimate the accuracy of peptide identifications made by MS/MS and database search. *Anal. Chem.* **2002**, *74* (20), 5383−92.

(24) Nesvizhskii, A. I.; Keller, A.; Kolker, E.; Aebersold, R. A statistical model for identifying proteins by tandem mass spectrometry. *Anal. Chem.* **2003**, *75* (17), 4646−58.

(25) Huang da, W.; Sherman, B. T.; Lempicki, R. A. Systematic and integrative analysis of large gene lists using DAVID bioinformatics resources. *Nat. Protoc.* **2009**, *4* (1), 44−57.

(26) Huang da, W.; Sherman, B. T.; Lempicki, R. A. Bioinformatics enrichment tools: paths toward the comprehensive functional analysis of large gene lists. *Nucleic Acids Res.* **2009**, *37* (1), 1−13.

(27) Bendtsen, J. D.; Nielsen, H.; von Heijne, G.; Brunak, S. Improved prediction of signal peptides: SignalP 3.0. *J. Mol. Biol.* **2004**, *340* (4), 783−95.

(28) Bendtsen, J. D.; Jensen, L. J.; Blom, N.; Von Heijne, G.; Brunak, S. Feature-based prediction of non-classical and leaderless protein secretion. *Protein Eng. Des. Sel.* **2004**, *17* (4), 349−56.

(29) Sonnhammer, E. L.; von Heijne, G.; Krogh, A. A hidden Markov model for predicting transmembrane helices in protein sequences. *Proc. Int. Conf. Intell. Syst. Mol. Biol.* **1998**, *6*, 175−82.

(30) Chang, K. P.; Chang, Y. T.; Liao, C. T.; Yen, T. C.; Chen, I. H.; Chang, Y. L.; Liu, Y. L.; Chang, Y. S.; Yu, J. S.; Wu, C. C. Prognostic cytokine markers in peripheral blood for oral cavity squamous cell carcinoma identified by multiplexed immunobead-based profiling. *Clin. Chim. Acta* **2011**, *412* (11−12), 980−7.

(31) Liu, H.; Sadygov, R. G.; Yates, J. R., 3rd A model for random sampling and estimation of relative protein abundance in shotgun proteomics. *Anal. Chem.* **2004**, *76* (14), 4193−201.

(32) Ginos, M. A.; Page, G. P.; Michalowicz, B. S.; Patel, K. J.; Volker, S. E.; Pambuccian, S. E.; Ondrey, F. G.; Adams, G. L.; Gaffney, P. M. Identification of a gene expression signature associated with recurrent disease in squamous cell carcinoma of the head and neck. *Cancer Res.* **2004**, *64* (1), 55−63.

(33) Peng, C. H.; Liao, C. T.; Peng, S. C.; Chen, Y. J.; Cheng, A. J.; Juang, J. L.; Tsai, C. Y.; Chen, T. C.; Chuang, Y. J.; Tang, C. Y.; Hsieh, W. P.; Yen, T. C. A novel molecular signature identified by systems genetics approach predicts prognosis in oral squamous cell carcinoma. *PLoS One* **2011**, *6* (8), e23452.

(34) Estilo, C. L.; O-charoenrat, P.; Talbot, S.; Socci, N. D.; Carlson, D. L.; Ghossein, R.; Williams, T.; Yonekawa, Y.; Ramanathan, Y.; Boyle, J. O.; Kraus, D. H.; Patel, S.; Shaha, A. R.; Wong, R. J.; Huryn, J. M.; Shah, J. P.; Singh, B. Oral tongue cancer gene expression profiling: Identification of novel potential prognosticators by oligonucleotide microarray analysis. *BMC Cancer* **2009**, *9*, 11.

(35) Pyeon, D.; Newton, M. A.; Lambert, P. F.; den Boon, J. A.; Sengupta, S.; Marsit, C. J.; Woodworth, C. D.; Connor, J. P.; Haugen, T. H.; Smith, E. M.; Kelsey, K. T.; Turek, L. P.; Ahlquist, P. Fundamental differences in cell cycle deregulation in human papillomavirus-positive and human papillomavirus-negative head/neck and cervical cancers. *Cancer Res.* **2007**, *67* (10), 4605−19.

(36) Talbot, S. G.; Estilo, C.; Maghami, E.; Sarkaria, I. S.; Pham, D. K.; P, O. c.; Socci, N. D.; Ngai, I.; Carlson, D.; Ghossein, R.; Viale, A.; Park, B. J.; Rusch, V. W.; Singh, B. Gene expression profiling allows distinction between primary and metastatic squamous cell carcinomas in the lung. *Cancer Res.* **2005**, *65* (8), 3063−71.

(37) Ye, H.; Yu, T.; Temam, S.; Ziober, B. L.; Wang, J.; Schwartz, J. L.; Mao, L.; Wong, D. T.; Zhou, X. Transcriptomic dissection of tongue squamous cell carcinoma. *BMC Genomics* **2008**, *9*, 69.

(38) Ogoshi, K.; Kasamatsu, A.; Iyoda, M.; Sakuma, K.; Yamatoji, M.; Sakamoto, Y.; Ogawara, K.; Shiiba, M.; Tanzawa, H.; Uzawa, K. Dickkopf-1 in human oral cancer. *Int. J. Oncol.* **2011**, *39* (2), 329−36.

(39) Shinohara, M.; Nakamura, S.; Harada, T.; Shimada, M.; Oka, M. Mode of tumor invasion in oral squamous cell carcinoma: improved grading based on immunohistochemical examination of extracellular matrices. *Head Neck* **1996**, *18* (2), 153−9.

(40) Sugiura, T.; Inoue, Y.; Matsuki, R.; Ishii, K.; Takahashi, M.; Abe, M.; Shirasuna, K. VEGF-C and VEGF-D expression is correlated with lymphatic vessel density and lymph node metastasis in oral squamous cell carcinoma: Implications for use as a prognostic marker. *Int. J. Oncol.* **2009**, *34* (3), 673−80.

(41) Yapijakis, C.; Bramos, A.; Nixon, A. M.; Ragos, V.; Vairaktaris, E. The interplay between hemostasis and malignancy: the oral cancer paradigm. *Anticancer Res.* **2012**, *32* (5), 1791−800.

(42) Mitra, R. S.; Zhang, Z.; Henson, B. S.; Kurnit, D. M.; Carey, T. E.; D'Silva, N. J. Rap1A and rap1B ras-family proteins are prominently expressed in the nucleus of squamous carcinomas: nuclear trans-

location of GTP-bound active form. *Oncogene* **2003**, *22* (40), 6243–56.
(43) Weng, L. P.; Wu, C. C.; Hsu, B. L.; Chi, L. M.; Liang, Y.; Tseng, C. P.; Hsieh, L. L.; Yu, J. S. Secretome-based identification of Mac-2 binding protein as a potential oral cancer marker involved in cell growth and motility. *J. Proteome Res.* **2008**, *7* (9), 3765–75.
(44) Moenner, M.; Pluquet, O.; Bouchecareilh, M.; Chevet, E. Integrated endoplasmic reticulum stress responses in cancer. *Cancer Res.* **2007**, *67* (22), 10631–4.
(45) Tsai, Y. C.; Weissman, A. M. The unfolded protein response, degradation from endoplasmic reticulum and cancer. *Genes Cancer* **2010**, *1* (7), 764–778.
(46) Lin, C. Y.; Chen, W. H.; Liao, C. T.; Chen, I. H.; Chiu, C. C.; Wang, H. M.; Yen, T. C.; Lee, L. Y.; Chang, J. T.; Cheng, A. J. Positive association of glucose-regulated protein 78 during oral cancer progression and the prognostic value in oral precancerous lesions. *Head Neck* **2010**, *32* (8), 1028–39.
(47) Ballar, P.; Pabuccuoglu, A.; Kose, F. A. Different p97/VCP complexes function in retrotranslocation step of mammalian ER-associated degradation (ERAD). *Int. J. Biochem. Cell Biol.* **2011**, *43* (4), 613–21.
(48) Guo, F.; Snapp, E. L. ERdj3 regulates BiP occupancy in living cells. *J. Cell Sci.* **2013**, *126* (Pt 6), 1429–39.
(49) Kamb, A. What's wrong with our cancer models? *Nat. Rev. Drug Discovery* **2005**, *4* (2), 161–5.
(50) Masters, J. R. Human cancer cell lines: fact and fantasy. *Nat. Rev. Mol. Cell Biol.* **2000**, *1* (3), 233–6.
(51) Hu, S.; Arellano, M.; Boontheung, P.; Wang, J.; Zhou, H.; Jiang, J.; Elashoff, D.; Wei, R.; Loo, J. A.; Wong, D. T. Salivary proteomics for oral cancer biomarker discovery. *Clin. Cancer. Res.* **2008**, *14* (19), 6246–52.
(52) Nagler, R.; Bahar, G.; Shpitzer, T.; Feinmesser, R. Concomitant analysis of salivary tumor markers—a new diagnostic tool for oral cancer. *Clin. Cancer. Res.* **2006**, *12* (13), 3979–84.
(53) Elashoff, D.; Zhou, H.; Reiss, J.; Wang, J.; Xiao, H.; Henson, B.; Hu, S.; Arellano, M.; Sinha, U.; Le, A.; Messadi, D.; Wang, M.; Nabili, V.; Lingen, M.; Morris, D.; Randolph, T.; Feng, Z.; Akin, D.; Kastratovic, D. A.; Chia, D.; Abemayor, E.; Wong, D. T. Prevalidation of salivary biomarkers for oral cancer detection. *Cancer Epidemiol. Biomarkers Prev.* **2012**, *21* (4), 664–72.
(54) Makawita, S.; Diamandis, E. P. The bottleneck in the cancer biomarker pipeline and protein quantification through mass spectrometry-based approaches: current strategies for candidate verification. *Clin. Chem.* **2010**, *56* (2), 212–22.
(55) Chen, Y. T.; Chen, H. W.; Domanski, D.; Smith, D. S.; Liang, K. H.; Wu, C. C.; Chen, C. L.; Chung, T.; Chen, M. C.; Chang, Y. S.; Parker, C. E.; Borchers, C. H.; Yu, J. S. Multiplexed quantification of 63 proteins in human urine by multiple reaction monitoring-based mass spectrometry for discovery of potential bladder cancer biomarkers. *J. Proteomics* **2012**, *75* (12), 3529–45.
(56) Krady, M. M.; Zeng, J.; Yu, J.; MacLauchlan, S.; Skokos, E. A.; Tian, W.; Bornstein, P.; Sessa, W. C.; Kyriakides, T. R. Thrombospondin-2 modulates extracellular matrix remodeling during physiological angiogenesis. *Am. J. Pathol.* **2008**, *173* (3), 879–91.
(57) Matos, A. R.; Coutinho-Camillo, C. M.; Thuler, L. C.; Fonseca, F. P.; Soares, F. A.; Silva, E. A.; Gimba, E. R. Expression analysis of thrombospondin 2 in prostate cancer and benign prostatic hyperplasia. *Exp. Mol. Pathol.* **2013**, *94* (3), 438–44.
(58) Chijiwa, T.; Abe, Y.; Inoue, Y.; Matsumoto, H.; Kawai, K.; Matsuyama, M.; Miyazaki, N.; Inoue, H.; Mukai, M.; Ueyama, Y.; Nakamura, M. Cancerous, but not stromal, thrombospondin-2 contributes prognosis in pulmonary adenocarcinoma. *Oncol. Rep.* **2009**, *22* (2), 279–83.
(59) Kodama, J.; Hashimoto, I.; Seki, N.; Hongo, A.; Yoshinouchi, M.; Okuda, H.; Kudo, T. Thrombospondin-1 and -2 messenger RNA expression in invasive cervical cancer: correlation with angiogenesis and prognosis. *Clin. Cancer. Res.* **2001**, *7* (9), 2826–31.
(60) MacLauchlan, S.; Yu, J.; Parrish, M.; Asoulin, T. A.; Schleicher, M.; Krady, M. M.; Zeng, J.; Huang, P. L.; Sessa, W. C.; Kyriakides, T. R. Endothelial nitric oxide synthase controls the expression of the angiogenesis inhibitor thrombospondin 2. *Proc. Natl. Acad. Sci. U.S.A.* **2011**, *108* (46), E1137–45.
(61) Oshika, Y.; Masuda, K.; Tokunaga, T.; Hatanaka, H.; Kamiya, T.; Abe, Y.; Ozeki, Y.; Kijima, H.; Yamazaki, H.; Tamaoki, N.; Ueyama, Y.; Nakamura, M. Thrombospondin 2 gene expression is correlated with decreased vascularity in non-small cell lung cancer. *Clin. Cancer. Res.* **1998**, *4* (7), 1785–8.
(62) Santin, A. D.; Zhan, F.; Bellone, S.; Palmieri, M.; Cane, S.; Bignotti, E.; Anfossi, S.; Gokden, M.; Dunn, D.; Roman, J. J.; O'Brien, T. J.; Tian, E.; Cannon, M. J.; Shaughnessy, J., Jr.; Pecorelli, S. Gene expression profiles in primary ovarian serous papillary tumors and normal ovarian epithelium: identification of candidate molecular markers for ovarian cancer diagnosis and therapy. *Int. J. Cancer* **2004**, *112* (1), 14–25.
(63) Rendtlew Danielsen, J. M.; Knudsen, L. M.; Dahl, I. M.; Lodahl, M.; Rasmussen, T. Dysregulation of CD47 and the ligands thrombospondin 1 and 2 in multiple myeloma. *Br. J. Hamaetol.* **2007**, *138* (6), 756–60.
(64) Horst, D.; Budczies, J.; Brabletz, T.; Kirchner, T.; Hlubek, F. Invasion associated up-regulation of nuclear factor kappaB target genes in colorectal cancer. *Cancer* **2009**, *115* (21), 4946–58.
(65) Reis, P. P.; Waldron, L.; Perez-Ordonez, B.; Pintilie, M.; Galloni, N. N.; Xuan, Y.; Cervigne, N. K.; Warner, G. C.; Makitie, A. A.; Simpson, C.; Goldstein, D.; Brown, D.; Gilbert, R.; Gullane, P.; Irish, J.; Jurisica, I.; Kamel-Reid, S. A gene signature in histologically normal surgical margins is predictive of oral carcinoma recurrence. *BMC Cancer* **2011**, *11*, 437.